

*Full Length Research Paper*

# Removal of phosphate ions from aqueous solutions using bauxite obtained from Mulanje, Malawi

Kamiyango, M. W.<sup>1</sup>, Sajidu, S. M. I.<sup>2\*</sup> and Masamba, W. R. L.<sup>3</sup>

<sup>1</sup>College of Medicine, University of Malawi, P/Bag 360, Chichiri, Blantyre 3, Malawi.

<sup>2</sup>Chemistry Department, Chancellor College, P.O. Box 280, Zomba, Malawi.

<sup>3</sup>Harry Oppenheimer, Okavango Research Centre, P/Bag 285, Maun, Botswana.

Accepted 20 June, 2011

Studies on stream water and effluent from selected wastewater treatment plants in Blantyre, Malawi, have reported phosphate concentrations above recommended levels. High phosphate levels in the effluent and streams pose a threat to aquatic life through the stimulation of excessive growth of plants and toxic cyanobacteria. Phosphate removal by bauxite was investigated as a function of pH, contact time, dosage, competing ions and initial phosphate concentration by means of jar tests. Phosphate removal increased with decreasing pH with maximum removal (99.75%) recorded at pH  $2.40 \pm 0.10$ . Phosphate removal was attributed to ligand exchange reactions with gibbsite and goethite minerals that are chemically and electrostatically favoured at low pH. Bauxite indicated a high phosphate removal capacity with 98.42% removal recorded for a dosage of 15 g/l. This was attributed to the presence of goethite and gibbsite minerals for which phosphate has a strong affinity. Kinetics studies revealed a fast adsorption reaction with 61 and 65% phosphate removal achieved after 30 min of contact at 20 and 40°C respectively. Phosphate removal was enhanced in the individual presence of calcium and magnesium ions whereas carbonate and sulphate ions reduced it by competing for active sites.

**Key words:** Adsorption, bauxite, phosphate, gibbsite, goethite, eutrophication.

## INTRODUCTION

Phosphorus is one of the primary nutrients that cause detrimental eutrophication in aquatic environments. A continuing elevated level of phosphorus in stagnant water systems stimulates growth of aquatic plants and toxic cyanobacteria. Phosphorus is found in wastewater mainly in the orthophosphate form and to a lesser extent in other forms that include polyphosphates and organically bound phosphates (Hammer and Hammer, 2001). Large quantities of phosphates are discharged into the aquatic environment through point sources such as domestic and industrial effluent, and also through non-point sources that include fertilizer rich runoff from agricultural lands. Total phosphorus content of effluents or streams that discharge directly into lakes and dams is regulated by national and international water standard authorities with

maximum limits ranging from 0.1 to 2.0 mg/l as P, with many established at 1.0 mg/l (Hammer and Hammer, 2001).

A study on water and wastewater quality in Blantyre, Malawi, revealed phosphate concentrations ranging from 0.63 to 5.50 mg/l in some streams and effluent from some wastewater treatment plants (Sajidu et al., 2007). The elevated phosphate levels indicate the need for efficient removal of phosphate ions during wastewater treatment to prevent the occurrence of eutrophication in the receiving water bodies. Biological uptake and chemical precipitation (using iron and aluminium salts), are the most established methods for phosphorus removal from wastewater. However, problems are encountered owing to poor operation stability or high economic costs respectively. As a result of the problems associated with the established methods, there has been a growing interest in search for cheap and abundant phosphate adsorbents. A lot of studies have been done on phosphate removal using low cost materials such as blast furnace slags (Johansson and Gustafsson, 2000;

\*Corresponding author. Email: [sajidu@chanco.unima.mw](mailto:sajidu@chanco.unima.mw), [ssajidu@yahoo.co.uk](mailto:ssajidu@yahoo.co.uk). Tel: +265 (0) 8 88 891 714. Fax: +265 (1) 524 046.

Kostura et al., 2005) alunite (Ozacar, 2006), calcite (Karageorgiou et al., 2007), iron oxide tailings (Zeng et al., 2004), flyash (Can and Yildiz, 2006; Chen et al., 2007), bauxsol (Akhurst et al., 2006), red mud (Huang et al., 2008; Pradhan et al., 1998) and sludge from Fuller's earth production (Moon et al., 2007). Removal of phosphate ions by the low cost materials was achieved through adsorption on iron and aluminium hydroxides or precipitation of calcium phosphate salts. Reactions between phosphate species and iron and aluminium salts during chemical precipitation are complex and not fully understood; however, the primary reaction appears to be the combining of orthophosphate ion with the metal cation (Hammer and Hammer, 2001). Investigations on phosphate removal using calcium containing materials such as fly ash and calcite have shown that phosphate precipitates with calcium as apatites, especially hydroxyapatites  $[\text{Ca}_5(\text{PO}_4)_3\text{OH}]$  (Johansson and Gustafsson, 2000; Karageorgiou et al., 2007; Moon et al., 2007).

Goethite ( $\alpha\text{-FeOOH}$ ) is a widely studied iron oxide mineral owing to its role in nutrient adsorption and desorption in soils. The mechanism of adsorption of phosphate on goethite was first reported by Russell et al. (1974). Recent studies on phosphate adsorption on goethite have provided further details on the types and properties of complexes formed. Adsorption of phosphate ions on goethite is attributed to a ligand exchange reaction on the adsorbent surface, in which phosphate is exchanged with surface structural hydroxyl groups (Russell et al., 1974). Specifically, phosphate adsorption on goethite proceed mainly via formation of inner sphere bidentate complexes,  $(\text{FeO})_2\text{PO}_2(\text{H})$  from pH 3.5 to 8.0 with abundance of a monodentate complex,  $\text{FeOPO}_3(\text{H})_{1,2}$ , increasing with increasing pH and decreasing phosphate surface coverage (Zhong et al., 2007). Similarly, phosphate adsorption on hematite proceeds through the formation of monodentate (bridging and mononuclear) complexes (Elzinga and Sparks, 2007). Aluminium oxide surfaces as well bind phosphate ions through the formation of ion-pairs or by a ligand exchange reaction mechanism (Goldberg et al., 1996).

This paper reports studies on the feasibility of the removal of phosphate species from aqueous solutions by locally available bauxite (containing goethite and gibbsite,  $\alpha\text{-Al}(\text{OH})_3$ ), obtained from deposits located in the district of Mulanje, Malawi.

## MATERIALS AND METHODS

### Preparation of bauxite samples

Bauxite samples used in this study were obtained from the district of Mulanje, Malawi. The bauxite is mainly a trihydrate gibbsite which lies over kaolinite and has free quartz and goethite as the main contaminants. Bauxite samples were sun-dried for 48 h and later ground to fine powder using a traditional mortar and pestle. The

ground bauxite was later passed through a 60-mesh size (BS) sieve to remove ungrounded particles. The fine bauxite powder prepared in this way was used throughout the study.

### Preparation of standard solutions

A standard phosphate stock solution (1000 mg/l) was prepared by dissolving an appropriate amount of analytical grade anhydrous  $\text{KH}_2\text{PO}_4$  (Glassworld, SA) in distilled water. Intermediate standard solutions (100 mg/l) were prepared by diluting the stock solution with distilled water. The intermediate standard solutions were used in obtaining desired phosphate concentrations. Similarly, carbonate standard solutions were prepared from  $\text{Na}_2\text{CO}_3$  (Glassworld, SA) whilst sulphate, calcium ( $\text{Ca}^{2+}$ ), and magnesium ( $\text{Mg}^{2+}$ ) standard solutions were prepared by dissolving anhydrous  $\text{Na}_2\text{SO}_4$  (ACE, SA),  $\text{Ca}(\text{NO}_3)_2$  (SAARCHEM, SA), and  $\text{Mg}(\text{NO}_3)_2$  (Glassworld, SA) salts, respectively, in distilled water. The background  $\text{NaNO}_3$  solution (0.1 mol/l) was prepared by dissolving a calculated amount of sodium nitrate (BDH) in distilled water.

### General batch adsorption procedure

Defined masses of bauxite were weighed into centrifuge tubes to which was added a defined volume of 0.1 mol/l  $\text{NaNO}_3$  electrolyte followed by a volume of 100 mg/l standard phosphate solution to make a total of 10 ml. Depending on the parameter under study, calculated volumes of chemical species of interest were added before introduction of the phosphate solution with adjustments made to the added volumes in order to obtain a total volume of 10 ml. An appropriate amount of nitric acid (0.02 mol/l) or sodium hydroxide (0.02 mol/l) was added to the bauxite suspension to adjust the pH to a certain value. The mixture was shook for a defined period of time using a Griffin flask shaker then centrifuged at 2500 rpm using a Hettich Roxita/AP centrifuge. The supernatant (2 to 3 ml) was then passed through a Titan, 0.45  $\mu\text{m}$  PES membrane filter to remove solid particles. A component suppression ion chromatography system composed of a Dionex CDM-1 conductivity detector, an Ionpac AS14 anion exchange column and Data Apex Clarity chromatography software, was used to determine phosphate concentration of the filtered supernatants. A Thermo Ross Sure Flow combination electrode (Orion 8172) along with a Mettler-Toledo SevenMulti meter was used throughout the study to determine the pH of the bauxite suspensions. The pH electrode was regularly calibrated with pH  $7.00 \pm 0.02$  and pH  $4.01 \pm 0.02$  buffer solutions (MettlerToledo).

### Effect of pH on phosphate uptake

Bauxite samples (0.05 g) were weighed in triplicate into acid washed 50 ml centrifuge tubes. An appropriate amount of nitric acid (0.02 mol/l) or sodium hydroxide (0.02 mol/l) was added to the weighed samples to adjust pH to a certain value. This was followed by thorough mixing and equilibration of the mixture for 20 min. Sodium nitrate and potassium dihydrogen phosphate solutions were then added to each centrifuge tube to obtain concentrations of 0.01 and 10 mg/l for sodium nitrate (electrolyte) and phosphate ions respectively. Mixtures prepared in this manner were shook at 200 rpm for 90 min and later centrifuged at 2500 rpm for 20 min. The supernatant was filtered through a 0.45  $\mu\text{m}$  membrane and analyzed for phosphate using ion chromatography.

### Studies of adsorption kinetics

A solution of phosphate ions (10 mg/l) was prepared in 0.01 mol/l

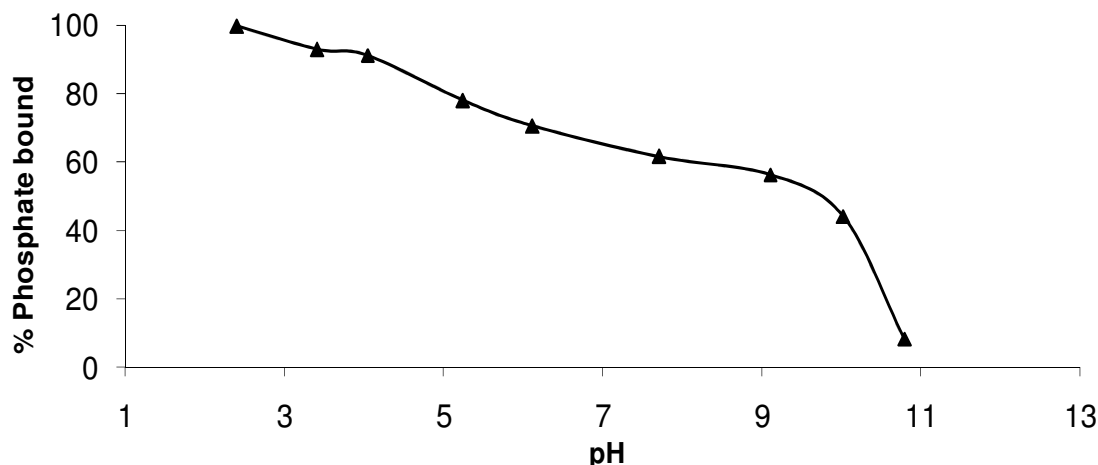


Figure 1. Plot of % phosphate bound against pH.

$\text{NaNO}_3$  electrolyte and equilibrated to 20 and 40°C in a temperature controlled water bath. This was followed by mixing of the equilibrated solutions (100 ml) with weighed bauxite samples to obtain a bauxite dosage of 5 g/l. Mixtures of bauxite and phosphate solution (in an electrolyte) were shook in a student's water bath (Gallenkamp Thermostirrer 85) equipped with a temperature control system at 200 rpm for 5 h. Small volumes of the suspension (0.5 ml) were withdrawn at intervals throughout the 5 h of contact time. The sample withdrawn at an interval (0.5 ml), was quickly passed through a 0.45  $\mu\text{m}$  membrane and injected into an ion chromatograph for phosphate analysis within a minute of sampling. The effect of increasing contact time was studied at 20 and 40°C to concurrently assess the effect of temperature on adsorption of phosphate by bauxite.

#### Effect of initial phosphate concentration on the phosphate uptake capacity of bauxite

Bauxite samples (0.05 g) were weighed in triplicate into acid washed centrifuge tubes. Intermediate phosphate solution (100 mg/l), and sodium nitrate (1.0 mol/l) electrolyte were made up to 10 ml with distilled water to obtain 0.01 mol/l sodium nitrate and initial phosphate concentrations for each triplicate of 5, 10, 15, 20, 30, 40, 50, and 60 mg/l. Each complete setup was prepared with solutions pre-equilibrated to different temperatures of 10, 20, 30, 40, 50 and 60°C. Mixtures prepared in this manner were shook at 200 rpm for 90 min at a specific temperature in a water bath and later centrifuged at 2500 rpm for 20 min. The supernatant obtained was later filtered through a 0.45  $\mu\text{m}$  membrane and analyzed for phosphate using ion chromatography.

#### Effect of the presence of magnesium, calcium, sulphate and carbonate ions in solution on phosphate uptake

Bauxite samples (0.05 g) were weighed in triplicate into acid washed 50 ml centrifuge tubes. A combination of solutions was prepared to obtain 10 mg/l initial phosphate concentration, 0.01 mol/l sodium nitrate electrolyte and competing ion ( $\text{Mg}^{2+}$ ,  $\text{Ca}^{2+}$ ,  $\text{SO}_4^{2-}$  or  $\text{CO}_3^{2-}$ ) concentrations of 0, 10, 20, 40, 60, 80, 100, 200, 300, and 500 mg/l. Phosphate was introduced last during the preparation of the mixtures to prevent reactions between phosphate and bauxite in the absence of the competing ion. The mixtures prepared in this manner were shook for 90 min and later

centrifuged at 2500 rpm for 20 min. The supernatant was filtered through a 0.45  $\mu\text{m}$  membrane and analyzed for phosphate using ion chromatography.

#### Multi-interactive effect of magnesium, calcium, sulphate, and carbonate ions on the phosphate removal efficiency of bauxite

Triplicate bauxite samples of masses 0.01, 0.03, 0.05, 0.1, 0.2, 0.3, 0.4, 0.5, 0.6, and 0.8 g were weighed into acid cleaned centrifuge tubes. To each tube, 2 ml of each solution of 1000 mg/l sodium carbonate, calcium nitrate, sodium sulphate, and magnesium nitrate were added followed by 1.4 ml of distilled water. Finally, 0.1 ml of sodium nitrate (1.0 mol/l) and 0.5 ml of phosphate solution (1000 mg/l) was added to each tube to obtain a total volume of 10 ml. The final composition of the solution was 50 mg/l phosphate, 0.01 mol/dm<sup>3</sup> sodium nitrate electrolyte, and 200 mg/l of sodium carbonate, calcium nitrate, sodium sulphate, and magnesium nitrate. Another set of triplicate bauxite samples was weighed into centrifuge tubes. To this set of bauxite samples was added the phosphate solution and the sodium nitrate electrolyte only with a final composition of 50 mg/l phosphate and 0.01 mol/dm<sup>3</sup> sodium nitrate background electrolyte. The second set of bauxite-phosphate mixtures acted as a control for the first set to which competing ions were added. Mixtures prepared in this manner were shook for 90 min and later centrifuged at 2500 rpm for 20 min. The supernatant was filtered through a 0.45  $\mu\text{m}$  membrane and analyzed for phosphate via ion chromatography.

## RESULTS AND DISCUSSION

### Effect of suspension pH

Variation of percent phosphate removal with initial suspension pH is shown in Figure 1. The reported percent phosphate removals were obtained using a bauxite dosage of 5.0 g/l, an initial phosphate concentration of 10.0 mg/l, and a contact time of 90 min. The percentage of phosphate ions bound by bauxite was determined from the ratio of phosphate ions present in the solution as given by Equation 1:

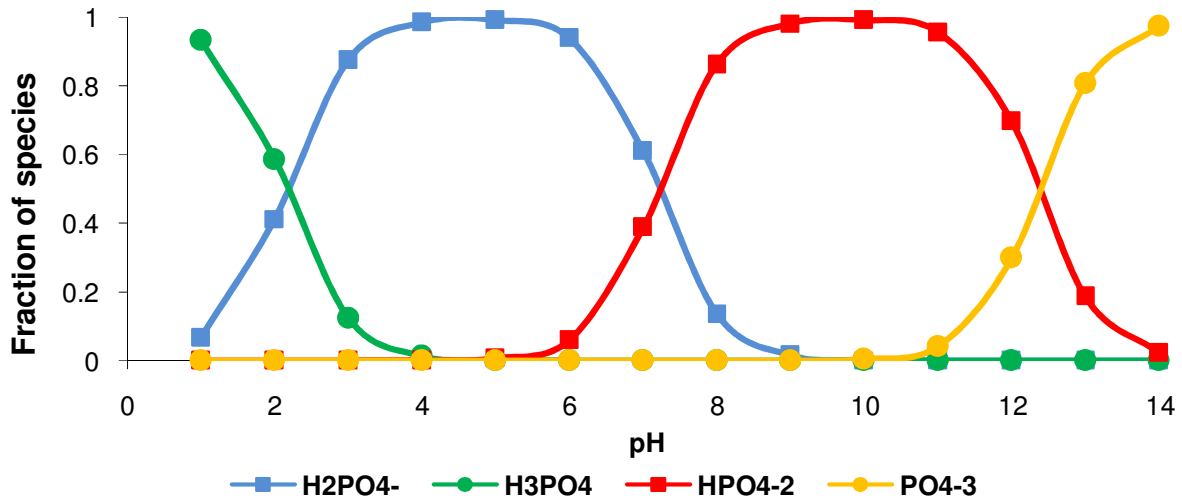


**Figure 2.** Fractional composition of phosphate species in the solution at different pH, calculated using the Visual Minteq program.

$$\% \text{ Phosphate removal} = \left( \frac{C_o - C_e}{C_o} \right) \times 100\% \quad (1)$$

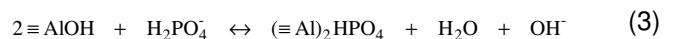
Where,  $C_o$  and  $C_e$  are the initial and equilibrium phosphate concentrations respectively, given in units of mg/l. The results obtained indicate that adsorption of phosphate on bauxite increases with decreasing pH, with the highest adsorption capacity (99.75%) obtained at pH  $2.40 \pm 0.10$  (the lowest pH used in this investigation). The amount of phosphate ions removed from solution by bauxite at equilibrium pH  $2.40 \pm 0.10$ , was more than double of that removed by bauxite at the equilibrium pH of  $10.03 \pm 0.11$  (99.75% compared to 44.01%). This observation can be attributed to the effects of solution pH on both phosphate speciation and charge development on the bauxite surface. Phosphate speciation in solutions of different pH was calculated using the Visual Minteq program and the results are indicated by Figure 2.

It can be noted from Figure 2 that the dominant phosphate species in solution at pH 2.40 was the singly charged ion,  $\text{H}_2\text{PO}_4^-$ , whereas the doubly charged ion,  $\text{HPO}_4^{2-}$ , was dominant at pH 10.03. The increase in phosphate adsorption with decreasing pH can be explained in part by the preferential adsorption of the singly charged phosphate species ( $\text{H}_2\text{PO}_4^-$ ) compared to the doubly charged ion,  $\text{HPO}_4^{2-}$ .

In general terms, adsorption of phosphate ions by bauxite can be attributed to the presence of two minerals, namely, gibbsite and goethite. This hypothesis is based on findings from various studies that indicate high affinity of phosphate ions for the gibbsite and goethite surfaces (Altundogan and Tumen, 2003; Arai and Sparks, 2001; Elzinga and Sparks, 2007; Hiemstra and van Riemsdijk, 1999; Horanyi and Joo, 2002; Kubicki et al., 2007; Persson et al., 1996; Pradhan et al., 1998; Rahnamaie et

al., 2007; Stachowicz et al., 2008; Zhong et al., 2007). Kaolinite was present in significant amounts in the bauxite samples as an impurity; however, it did not significantly contribute toward the high phosphate removal capacity of bauxite as it is poor at binding phosphate (Kamiyango et al., 2009). Besides having a low phosphate removal capacity, the pH dependency of phosphate adsorption on kaolinite is marked by the presence of an adsorption envelope with maxima between pH 4 and 6. Such an adsorption envelope is absent in Figure 1, indicating that kaolinite was not mainly responsible for the recorded high phosphate removals.

The effect of solution pH on adsorption of phosphate on goethite and gibbsite is explained by the acid-base properties of the active functional groups in the two minerals. Adsorption of phosphate ions on gibbsite is guided by the amphoteric aluminol functional group,  $\equiv\text{AlOH}$ , located on crystal edges. Adsorption of phosphate ions on gibbsite can be explained by the formation of inner sphere complexes between phosphate and the singly coordinated hydroxyl groups (Goldberg et al., 1996). Complexation of phosphate ions on the gibbsite surface via ligand exchange reaction mechanisms can be represented by Equations 2 and 3 for monodentate and bidentate phosphate bonding respectively:



Formation of phosphate complexes on iron oxides has been widely studied using spectroscopic techniques, radiotracer studies, and quantum chemical calculations

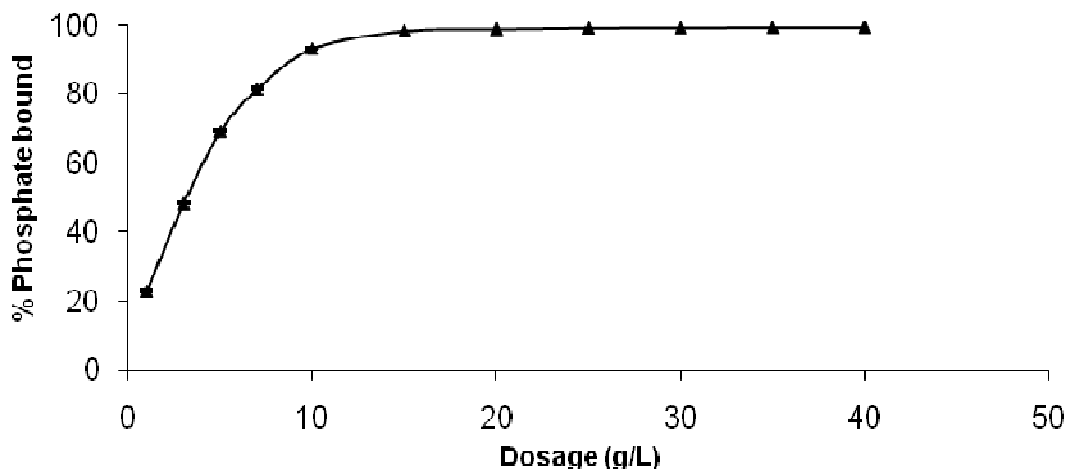
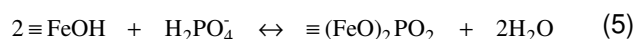


**Figure 3.** Plot of percentage of phosphate removal against dosage.

(Arai and Sparks, 2001; Elzinga and Sparks, 2007; Hiemstra and van Riemsdijk, 1999; Horanyi and Joo, 2002; Kubicki et al., 2007; Persson et al., 1996; Rahnamaie et al., 2007; Stachowicz et al., 2008; Zhong et al., 2007). The primary charging behaviour and adsorption reactions between goethite and ionic species in solution is attributed to the singly ( $\equiv\text{FeOH}(\text{OH})$ ) and triply ( $\equiv\text{Fe}_3\text{O}(\text{H})$ ) coordinated surface oxygens located on the dominant 110 crystal face (Hiemstra and van Riemsdijk, 1996). Ligand exchange reactions on the goethite surface involving the singly coordinated hydroxyl groups can therefore be represented by Equations 4 and 5, for monodentate and bidentate phosphate bonding respectively:



Dependency of phosphate adsorption on solution pH is further indicated by an abrupt decline in the amount of phosphate ions adsorbed on bauxite between pH 9 and 10. This abrupt decline can be explained by the charging behaviour of gibbsite and goethite under different pH conditions. Gibbsite has a point of zero net proton charge (p.z.n.p.c.) value of around 9.8 (Hiemstra and Van Riemsdijk, 1999), as such, the aluminol functional groups attain a net positive charge below pH 9.8, and a net negative charge above pH 9.8. Phosphate adsorption on gibbsite is therefore favoured below the p.z.n.p.c. as a result of electrostatic and chemical attraction to the positively charged gibbsite surface. The development of a net negative charge above the p.z.n.p.c. introduces electrostatic repulsions between the negatively charged phosphate ions and the gibbsite surface and hence, a reduction in the amount of phosphate ions bound. The

same argument can be extended to goethite with reported p.z.n.p.c. values of around 9.25 (Rietra et al., 2001).

#### **Effect of dosage on the phosphate removal capacity of bauxite**

Figure 3 indicates the effect of increasing bauxite dosage on percent removal of phosphate ions. The reported percent phosphate removals were obtained using an initial phosphate concentration of 10.0 mg/l, a contact time of 90 min, and a suspension pH of  $6.21 \pm 0.11$  (pH of bauxite suspension without adjustments).

The amount of phosphate bound by bauxite increased steadily with increasing dosage starting from the dosage of 1 g/l up to 15 g/l. This was followed by a gradual increase beyond 15 g/l as phosphate removal approached 100% (98.42% for the dosage of 15 g/l).

The increase in the amount of phosphate ions bound with increasing bauxite dosage can be attributed to an increase in the number of active sites available on both goethite and gibbsite. Studies on the removal of phosphate ions by red mud (Huang et al., 2008; Pradhan et al., 1998), iron oxide tailings (Zheng et al., 2004), bauxsol (Arkhurst et al., 2006), and alunite (Ozacar, 2006), reported effective adsorbent dosages ranging from, 10 to 20 g/l. These dosages were recorded for various initial phosphate concentrations ranging from 10 to 100 mg/l. The phosphate removal capacity of bauxite used in this study is comparable to that of red mud, iron oxide tailings, bauxsol, and alunite, even though a lower initial phosphate concentration of 10 mg/l was used.

#### **Kinetics of adsorption of phosphate ions on bauxite**

The effect of contact time on the amount of phosphate

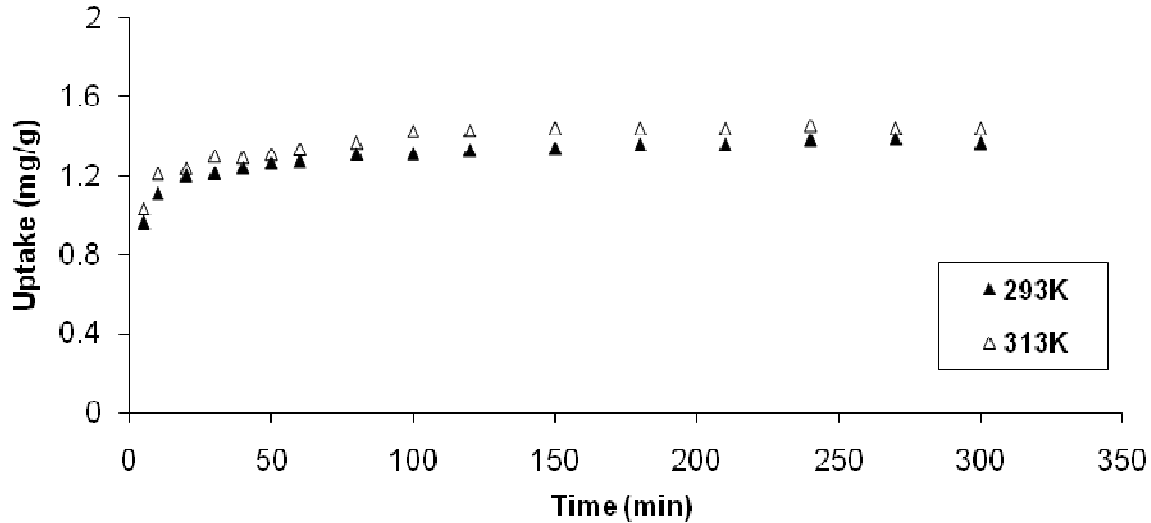


**Figure 4.** Plot of phosphate uptake against time for phosphate adsorption on bauxite.

ions adsorbed on bauxite is shown in Figure 4. Phosphate uptake (mg/g) was calculated as the ratio of

phosphate ions adsorbed to the mass of bauxite used as given by Equation 6:

$$\text{Phosphate uptake (mg/g)} = \left( \frac{C_o - C_e}{\text{Dosage (g)}} \right) \times \text{Sample volume (L)} \quad (6)$$

Where,  $C_o$  and  $C_e$  are the initial and equilibrium phosphate concentrations respectively, given in units of mg/l. The changes in phosphate adsorption with increasing contact time were obtained for a fixed bauxite dosage of 5 g/l, initial phosphate concentration of 10 mg/l, and bauxite suspension pH of  $6.21 \pm 0.11$ .

It is shown in Figure 4 that much of the adsorption occurred after 30 min of contact (61 and 65% phosphate removal at 20 and 40°C respectively). Faster reactions were also reported for adsorption of phosphate ions on iron oxide tailings (Zheng et al., 2004), as well as on alunite (Ozacar, 2006). Adsorption of phosphate ions on metal oxides proceed through a fast reaction stage lasting a few hours, followed by a slow reaction that can last for months to reach equilibrium (Barrow, 1999). Kinetics studies that are performed for a few hours provide information about the faster stage of the reaction, as it were the case in this study. A faster reaction between phosphate ions and the adsorbent is of primary importance in the application of metal oxides as adsorbents for wastewater treatment considering that shorter contact times would be required. Figure 4 further indicates that the reaction rate was not significantly affected by temperature. As the adsorption reaction is fairly rapid, the effects of temperature are mainly seen on the position of its equilibrium, rather than on its rate (Barrow, 1999).

The kinetic mechanism of phosphate uptake was evaluated with two different models: the Lagergren pseudo first order and pseudo second order models (Huang et al., 2008). The pseudo first order equation (Equation 7) takes the form:

$$\log(q_e - q_t) = \log q_e - \frac{k_1 t}{2.303} \quad (7)$$

Where,  $q_t$  is the amount of phosphate removed at time  $t$  (mg/g),  $q_e$  is the amount of phosphate bound at equilibrium (mg/g), and  $k_1$  is the equilibrium rate constant for pseudo first-order kinetics ( $s^{-1}$ ). The pseudo second-order equation (Equation 8) is expressed as:

$$\frac{t}{q_t} = \frac{1}{k_2 q_e^2} + \frac{t}{q_e} \quad (8)$$

Where,  $k_2$  is the equilibrium rate constant for the second-order kinetics ( $g \text{ mg}^{-1} \text{ s}^{-1}$ ).

Data obtained at 20 and 40°C fitted better to the pseudo second-order model than to the pseudo first-order model as indicated by  $R^2$  values shown in Figures 5 and 6

Rate constants for adsorption of phosphate ions on bauxite were calculated as  $2.747 \times 10^{-3}$  and  $2.982 \times 10^{-3}$

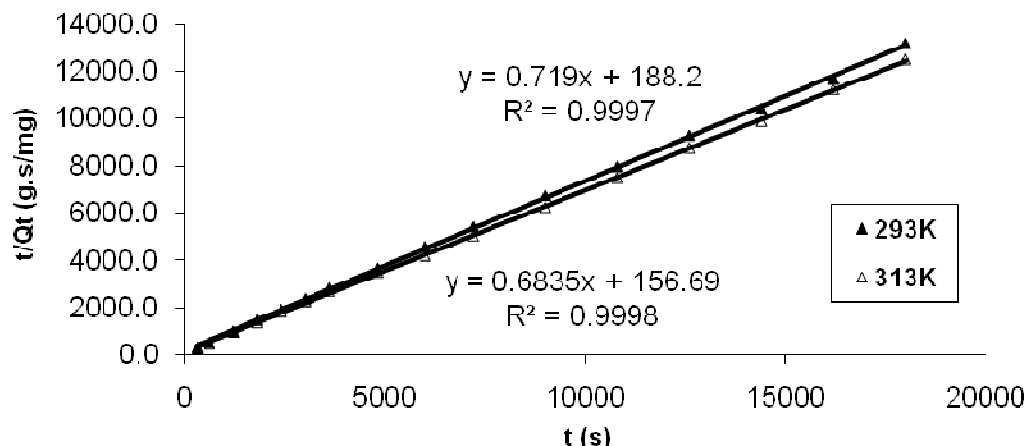


Figure 5. Second order fits for phosphate adsorption on bauxite.

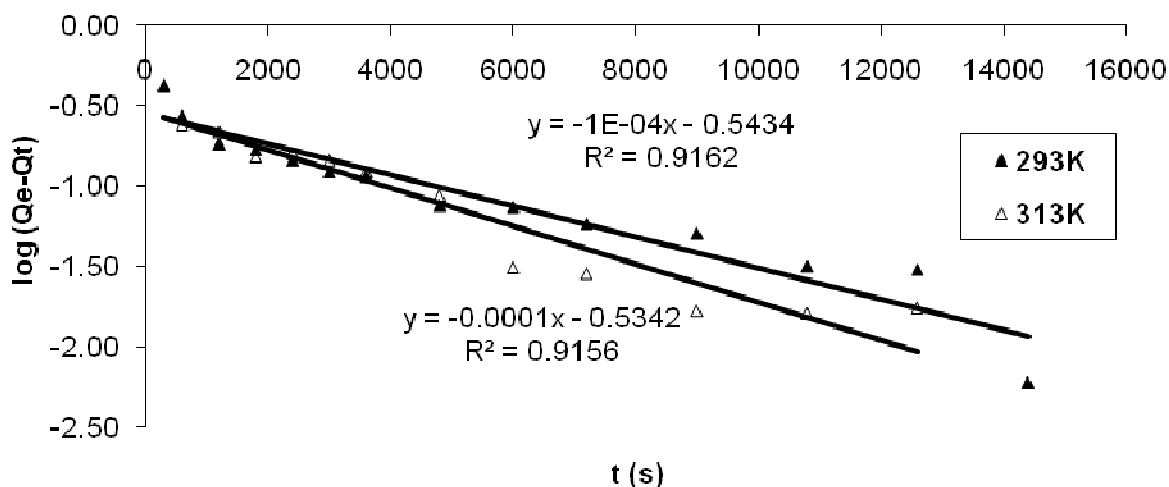


Figure 6. First order fits for phosphate adsorption on bauxite.

g/mg.s at 20 and 40°C respectively. The rate constant for the reaction at 40°C was slightly higher than that calculated for the reaction at 20°C. This slight difference further indicates that phosphate adsorption was least affected by temperature. The value of the activation energy of a reaction can be an important clue to the mechanism of a reaction (Barrow, 1999). Activation energy ( $E_a$ ) for phosphate adsorption on bauxite can be calculated using Equation 9:

$$\ln\left(\frac{k_{2(a)}}{k_{2(b)}}\right) = \frac{E_a}{R} \left(\frac{1}{T_b} - \frac{1}{T_a}\right) \quad (9)$$

Where,  $k_{2(a)}$  and  $k_{2(b)}$  are second order equilibrium constants at 20 and 40°C respectively,  $T_a$  and  $T_b$  are temperatures in Kelvin and R is the universal gas

constant (8.314 J/K.mol). Lower activation energy of 3.130 kJ/mol was calculated for phosphate adsorption on bauxite compared to 76.56 kJ/mol calculated for phosphate removal by kaolinite as reported from a related study (Kamiyango et al., 2009). The lower activation energy for bauxite further indicates stronger affinity of metal hydroxides surfaces for phosphate ions in solution compared to favourability of other phosphate removal mechanisms such precipitation (phosphate removal mechanism reported for impure kaolinite) (Kamiyango et al., 2009).

#### Effect of initial phosphate concentration on the phosphate uptake capacity of bauxite

The effect of increasing initial phosphate concentration on phosphate uptake by bauxite was studied at tempe-

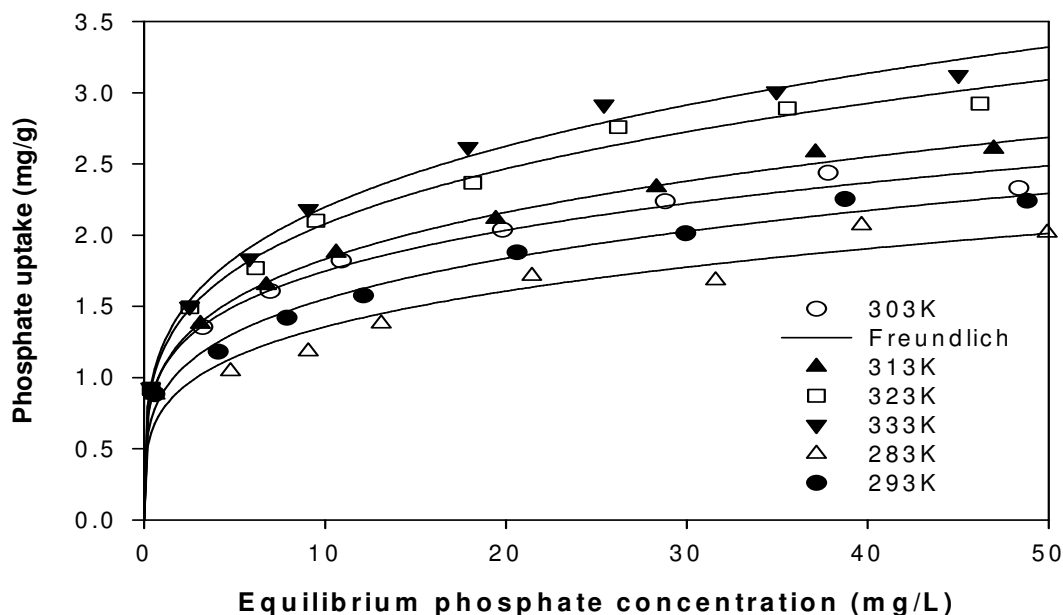


Figure 7. Phosphate uptake by bauxite fitted to the Freundlich equation.

Table 1. Equilibrium constants and Gibb's free energy change values.

Temperature (K)	$K_f$ ( $\text{dm}^3 \text{g}^{-1}$ )	$R^2$	$K_p$	$\Delta G$ ( $\text{kJmol}^{-1}$ )
283	0.7698	0.9132	769.8	-15.64
293	0.8864	0.9818	886.4	-16.53
303	1.054	0.9832	1053.6	-17.53
313	1.057	0.9961	1056.7	-18.12
323	1.178	0.9894	1177.7	-18.99
333	1.215	0.9907	1214.7	-19.66

atures of 10, 20, 30, 40, 50 and 60°C using a fixed dosage of 5 g/l and a contact time of 90 min. The pH of the bauxite suspensions was maintained around  $6.21 \pm 0.11$ . It can be seen from Figure 7 that phosphate uptake increased rapidly with increasing equilibrium phosphate concentration from 0 up to around 15 mg/l at all temperatures followed by a gradual increase beyond 15 mg/l. The rapid increase in phosphate uptake below 15 mg/l could be as a result of availability of excess active sites that later became saturated with further increase in phosphate concentration. This resulted in a gradual increase in phosphate uptake beyond 15mg/l.

Phosphate uptake at the studied temperatures was fitted to the Freundlich equation (Figure 7) by means of non-linear regression performed using Sigma plot software. The Freundlich equation is a semi-empirical model used to describe adsorption on heterogeneous systems (Milonjic, 2007):

$$q_e = K_f C_e^{\frac{1}{n}} \quad (10)$$

Where,  $K_f$  is the Freundlich constant ( $\text{dm}^3 \text{g}^{-1}$ ) and  $1/n$  is the heterogeneity factor. The data fitted well to the Freundlich equation as indicated by a minimum  $R^2$  value of 0.9132 obtained for the 283K system (Table 1). The Freundlich constant values  $K_f$ , obtained at each temperature were converted to dimensionless equilibrium constant values (Milonjic, 2007). The equilibrium constants,  $K_p$ , were used to calculate the Gibbs free energy change of adsorption  $\Delta G_{ad}$ , at each temperature (Table 1) using Equation 11:

$$\Delta G = -RT \ln K \quad (11)$$

Negative  $\Delta G$  values were obtained for phosphate adsorption on bauxite (Table 1) providing thermodynamic evidence that the adsorption process was spontaneous. The calculated  $\Delta G$  values became more negative with increasing temperature indicating an increase in thermodynamic favourability of the adsorption process. The enthalpy change of the reaction ( $\Delta H$ ), was estimated using the Van't Hoff equation (Atkins, 1990), given as:

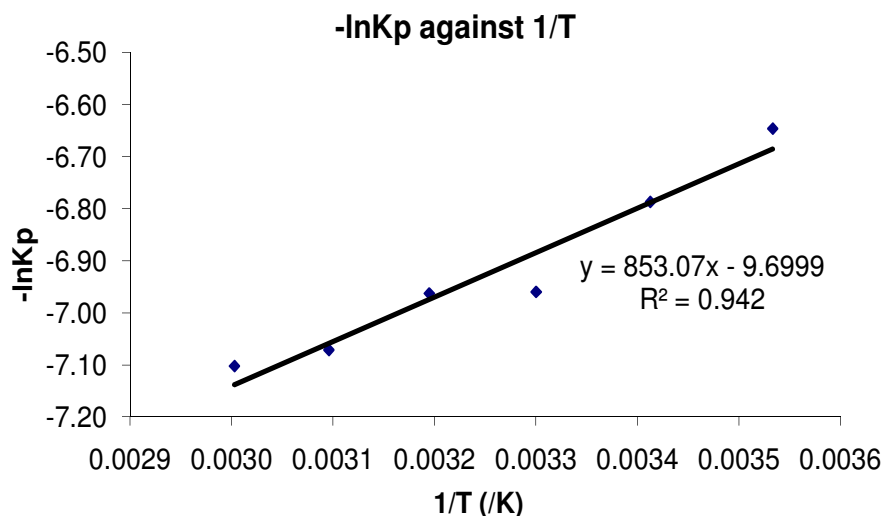


Figure 8. Vant Hoff plot for phosphate adsorption on bauxite.

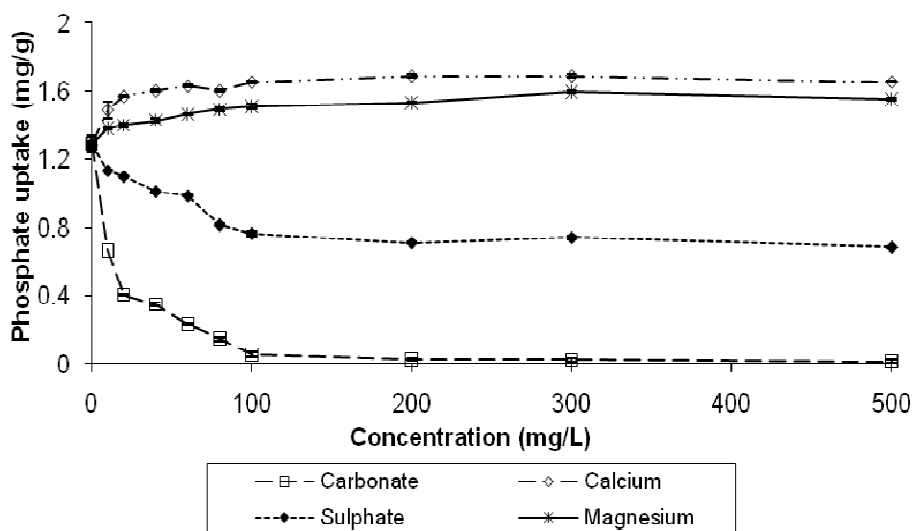


Figure 9. Effect of competing ions on adsorption of phosphate ions on bauxite.

$$\frac{d \ln K}{d(1/T)} = \frac{-\Delta H^{\circ}}{R} \quad (12)$$

Where, K is an equilibrium constant, T is the temperature (K), R is the universal gas constant ( $8.314 \text{ JK}^{-1}\text{mol}^{-1}$ ), and  $\Delta H^{\circ}$  is the standard reaction enthalpy. The enthalpy change of a reaction,  $\Delta H$ , was calculated from the slope of a plot of  $-\ln K_p$  against  $1/T$  (Atkins, 1990).  $\Delta H$  for phosphate adsorption on bauxite was estimated to be  $+6.943 \text{ kJmol}^{-1}$  (Figure 8), indicating that the process was endothermic, as such, adsorption of phosphate ions would increase with increasing temperature.

#### Effect of the presence of magnesium, calcium, sulphate and carbonate ions on removal of phosphate ions

Figure 9 shows the effect of magnesium, calcium, sulphate, and carbonate ions on the amount of phosphate ions bound on bauxite. It can be noted from the figure that phosphate uptake increased in the presence of magnesium and calcium ions, and decreased in the presence of sulphate and carbonate ions.

The observed increase in phosphate adsorption in the presence of calcium and magnesium ions can be

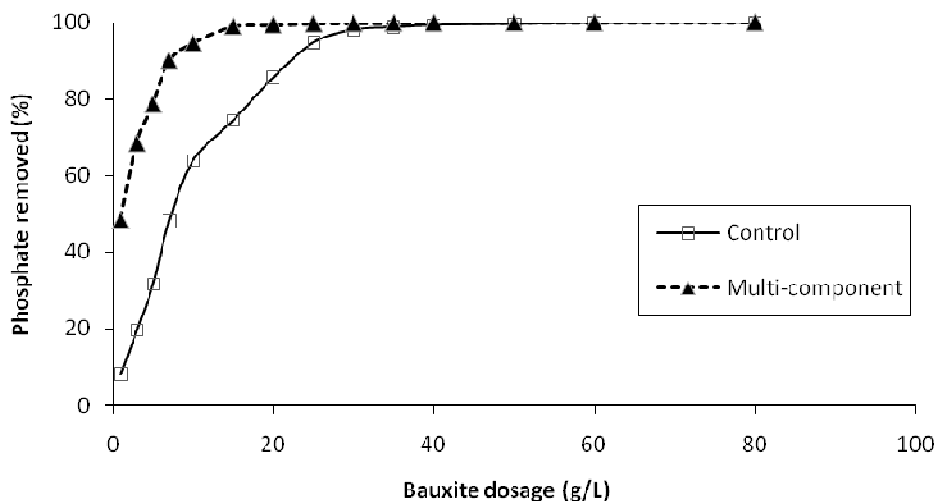


**Figure 10.** Multi-competitive effect of calcium, magnesium, carbonate, and sulphate ions on phosphate adsorption on bauxite.

explained by electrostatic interactions induced by the presence of the metal ions (Rietra et al., 2001). The negative charge of the adsorbed phosphate ions stimulates the binding of the positively charged calcium and magnesium ions and this suppresses an increase in negative charge (arising from the adsorption of phosphate ions) with suggested mutual effects of increased adsorption of both phosphate and the cations (Stachowicz et al., 2008). It can be noted from Figure 9 that the increase in phosphate adsorption in the presence of magnesium was smaller as compared to the increase in the presence of calcium. Magnesium adds less charge to the 1-plane (as depicted in the electrostatic double layer model) hence the small effect on phosphate adsorption since the mutual interaction between adsorbed cations and anions mainly stems from the charge attribution to this electrostatic plane (Stachowicz et al., 2008).

Figure 9 further indicates that carbonate ions strongly reduced the amount of phosphate ions adsorbed on bauxite. Carbonate ions forms a wide range of inner- and outer-sphere complexes with goethite and other metal hydroxides such as hematite as well as gibbsite (Hiemstra et al., 2004; Kubicki et al., 2007; Rahnemaie et al., 2007). Carbonate ions compete with phosphate for surface sites (owing to the formation of carbonate complexes with the metal (hydroxide surfaces) leading to a decrease in the adsorption of phosphate. Rahnemaie et al. (2007) noted that the competitive interaction of carbonate decreases as the pH increases and is very weak above pH 10.5, with maximum adsorption in closed systems occurring around pH 6-7. The observed strong competitive effect of carbonate in this study is justified by the pH conditions that were used of approximately  $6.21 \pm 0.112$  for which maximum carbonate adsorption is expected. The presence of carbonate in wastewater in

concentrations relatively higher than phosphate would greatly reduce the phosphate uptake efficiency of the bauxite as such proper measures would be required to mitigate the negative effects.

Sulphate ions competed weakly for active sites with phosphate ions (compared to carbonate) resulting in reduced phosphate uptake (Figure 9). Sulphate binding on iron hydroxide surfaces can be described by the formation of either monodentate or bidentate inner-sphere complexes through bridging mechanisms that are possibly dependent upon mineral surface loading (Kubicki et al., 2007). Sulphate has a weaker affinity for metal hydroxide surfaces as compared to phosphate such that no sulphate is adsorbed above the point of zero charge of goethite (Geelhoed et al., 1997). In sulphate-phosphate ion systems, presence of sulphate causes a small decrease in phosphate adsorption at relatively low pH (Geelhoed et al., 1997), which explains the weaker competition observed in this study.

#### **Multi-interactive effect of magnesium, calcium, sulphate, and carbonate ions on the phosphate removal efficiency of bauxite**

Figure 10 shows the multi-interactive effect of calcium, magnesium, sulphate, and carbonate ions on phosphate uptake by bauxite. An initial phosphate concentration of 50 mg/l and competing ion concentrations of 200 mg/l were used. In the control system, 50 mg/L of phosphate solution (in  $0.01 \text{ mol.dm}^{-3} \text{ NaNO}_3$ ) was treated with various bauxite dosages (up to a maximum of 80 g/l) for a period of 90 min. It is noted from Figure 10 that the presence of competing ions enhanced phosphate removal, that is, 98.93% removal obtained for the dosage of 15 g/l in the multi-component system compared to

74.43% in the control system.

The presence of carbonate and sulphate ions (200 mg/l) was expected to provide high competition for adsorption sites with phosphate ions even in the presence of calcium and magnesium ions (200 mg/l). This hypothesis is based on the understanding that enhancement of phosphate adsorption by calcium and magnesium ions as a result of electrostatic interactions is smaller in magnitude compared to the competitive effect of sulphate and carbonate ions. In an attempt to explain the observed enhancement of phosphate uptake in the multi-component system, the Visual Minteq program was used to calculate saturation index values of possible solid phases that could be precipitated. The results indicated that the system was saturated with respect to calcite (SI = 2.539), dolomite (SI = 5.584), hydroxyapatite (SI = 17.439), and magnesite (SI = 1.808) at a pH of  $8.452 \pm 0.2041$ . Mass distribution calculations indicated that 99.68% of calcium, 83.53% of carbonate, 63.15% of magnesium, 97.02% of phosphate, and 0.000% of sulphate ions would precipitate in the multi-component system. With 83.53% of carbonate and 0.000% of sulphate ions precipitated, there would still be a higher concentration of carbonate and sulphate ions to offer phosphate ions stiff competition for adsorption sites. Despite the presence of a higher concentration of competing ions, 97.02 % of phosphate ions would precipitate mainly as hydroxyapatite greatly reducing phosphate concentration in the process. Using results from the Visual Minteq calculations, the observed enhancement of phosphate removal in the multi-component system (Figure 10) was due to precipitation of phosphate ions as hydroxyapatite.

The optimum bauxite dosage for the multi-component system can be estimated to be in the range of 20 to 30 g/l. The optimum dosage estimated through the bench studies cannot be directly applied for wastewater treatment systems owing to differences in composition of the water as well as means of mechanical mixing of the bauxite and the wastewater. Rigorous shaking is involved during bench studies that might result in ripping of the bauxite particles and exposure of extra surface area containing reactive functional groups. Estimation of optimum dosage for use during wastewater treatment would require a pilot study and knowledge of the average chemical and physical composition of the influent wastewater.

## Conclusion

Results from this study have indicated that bauxite has a higher phosphate removal capacity owing to the presence of gibbsite and goethite. A fast reaction between phosphate and bauxite was recorded with 61 and 65% phosphate removal achieved after 30 min of contact at temperatures of 20 and 40 °C respectively. A

faster reaction between phosphate and bauxite would ensure shorter contact times during wastewater treatment. Despite having a higher phosphate removal capacity, the presence of carbonate and sulphate ions in higher concentrations would reduce the phosphate removal efficiency of bauxite. This negative effect would however be mitigated if the system is oversaturated with respect to some solid phases, in which case removal of phosphate ions would be achieved through other mechanisms other than adsorption. Determination of optimum bauxite dosages for the wastewater treatment plants would therefore require a pilot study that would consider factors such as mode of mechanical mixing, variations in influent composition in relation to dosage adjustments, sludge disposal and recycling.

## ACKNOWLEDGEMENTS

The authors acknowledge the support from the International Science Program (ISP) through International Programme in Chemical Sciences (IPICS) at the University of Uppsala, Sweden (project code MAW:02) for a grant that provided the MSc scholarship for Moses Kamiyango to study in the Chemistry Department of the University of Malawi.

## REFERENCES

- Akhurst DJ, Jones GB, Clark M, McConchie D (2006). Phosphate removal from aqueous solutions using neutralized bauxite refinery residues (Bauxsol). *Environ. Chem.* 3: 65-74.
- Altundogan HS, Tümen F (2003). Removal of phosphates from aqueous solutions. *J. Chem. Technol. Biotechnol.* 78 (7): 824-833.
- Arai Y, Sparks DL (2001). ATR-FTIR spectroscopic investigation on phosphate adsorption mechanisms at the ferrihydrite-water interface. *J. Colloid Interface Sci.* 241: 317-326.
- Atkins PW (1990). *Physical chemistry*. Oxford University press, 142-144.
- Barrow NJ (1999). The four laws of soil chemistry: the Leeper lecture 1998. *Aust. J. Soil Res.* 37: 787-829.
- Can MY, Yildiz E (2006). Phosphate removal from water by fly ash: Factorial experimental design. *J. Hazard. Mater. B.* 35: 165-170.
- Chen J, Kong H, Wu D, Chen X, Zhang D, Sun Z (2007). Phosphate immobilization from aqueous solution by fly ashes in relation to their composition. *J. Hazard. Mater. B* 139: 293-300.
- Elzinga JE, Sparks DL (2007). Phosphate adsorption onto hematite: An in situ ATR-FTIR investigation of the effects of pH and loading level on the mode phosphate surface complexation. *J. Colloid Interface Sci.* 308: 53-70.
- Geelhoed JS, Hiemstra T, van Riemsdijk WH (1997). Phosphate and sulphate adsorption on goethite: single anion and competitive adsorption. *Geochim. Cosmochim. Acta.* 61 (12): 2389-2396.
- Goldberg S, Davis JA, Hem JD (1996). The surface chemistry of aluminum oxides and hydroxides, in: Sposito, G. (Ed.), *The environmental chem. aluminum*. Lewis pub., Florida. 271-318.
- Hammer MJ, Hammer Jr (2001). *Water and wastewater technology*, 4<sup>th</sup> Ed. Prentice Hall, 234.
- Hiemstra T, Rahnemaie R, van Riemsdijk WH (2004). Surface complexation of carbonate on goethite: IR spectroscopy, structure and charge distribution. *J. Colloid Interface Sci.* 278: 282-290.
- Hiemstra T, van Riemsdijk WH (1996). A surface structural approach to ion adsorption: The charge distribution (CD) model. *J. Colloid Interface Sci.* 179: 488-508.

- Hiemstra T, van Riemsdijk WH (1999). Surface structural ion adsorption modelling of competitive binding of oxyanions by metal (hydr)oxides. *J. Colloid Interface Sci.* 210: 182-193.
- Horanyi G, Joo P (2002). Some peculiarities in the specific adsorption of phosphate ions on hematite and  $\gamma$ -Al<sub>2</sub>O<sub>3</sub> as reflected by radiotracer studies. *J. Colloid Interface Sci.* 247: 12-17.
- Huang W, Wang S, Zhu Z, Li L, Yao X, Rudolph V, Haghseresht F (2008). Phosphate removal from wastewater using red mud. *J. Hazard. Mater. B.* 158: 35-42.
- Johansson L, Gustafsson JP (2000). Phosphate removal using blast furnace slags and opoka-mechanisms. *Water Res.* 34(1): 259-265.
- Kamiyango MW, Masamba WRL, Sajidu SMI, Fabiano E (2009). Phosphate removal from aqueous solutions using kaolinite obtained from Linthipe, Malawi. *Phys. Chem. Earth A/B/C.* 34(13-16): 850-856.
- Karageorgiou K, Paschalis M, Anastassakis GN (2007). Removal of phosphate species from solution by adsorption onto calcite used as natural adsorbent. *J. Hazard. Mater. A.* 139: 447-452.
- Kostura B, Kulveitova H, Lesko J (2005). Blast furnace slags as sorbents of phosphate from water solutions. *Water Res.* 39: 1795-1802.
- Kubicki JD, Kwon KD, Paul KW, Sparks DL (2007). Surface complex structures modelled with quantum chemical calculations: carbonate, phosphate, sulphate, arsenate and arsenite. *Eur. J. Soil Sci.* 58: 932-944.
- Milonjic SK (2007). A consideration of the correct calculation of the thermodynamic parameters of adsorption. *J. Serb. Chem. Soc.* 72(12): 1363-1367.
- Moon YH, Kim JG, Ahn JS, Lee GG, Moon H (2007). Phosphate removal using sludge from fuller's earth production. *J. Hazard. Mater.* 143: 41-48.
- Ozacar M (2006). Contact time optimization of two-stage batch adsorber design using second-order kinetic model for the adsorption of phosphate onto alunite. *J. Hazard. Mater. B.* 137: 218-225.
- Persson P, Nilsson N, Sjöberg S (1996). Structure and bonding of orthophosphate ions at the iron oxide-aqueous interface. *J. Colloid Interface Sci.* 177: 263-275.
- Pradhan J, Das J, Das S, Thakur RS (1998). Adsorption of phosphate from aqueous solution using activated red mud. *J. Colloid Interface Sci.* 204: 169-172.
- Rahnemaie R, Hiemstra T, van Riemsdijk WH (2007). Carbonate adsorption on goethite in competition with phosphate. *J. Colloid Interface Sci.* 315: 415-425.
- Rietra RPJJ, Hiemstra T, van Riemsdijk WH (2001). Interaction between calcium and phosphate adsorption on goethite. *Environ. Sci. Technol.* 35 (16): 3369-3374.
- Russell JD, Parfitt RL, Fraser AR, Farmer VC (1974). Surface structures of gibbsite goethite and phosphated goethite. *Nature.* 248: 220-221.
- Sajidu SMI, Masamba WRL, Henry EMT, Kuyeli SM (2007). Water quality assessment in streams and wastewater treatment plants of Blantyre, Malawi. *Phys. Chem. Earth.* 32: 1391-1398.
- Stachowicz M, Hiemstra T, van Riemsdijk WH (2008). Multi-competitive interaction of As(III) and As(V) oxyanions with Ca<sup>2+</sup>, Mg<sup>2+</sup>, PO<sub>4</sub><sup>3-</sup>, and CO<sub>3</sub><sup>2-</sup> ions on goethite. *J. Colloid Interface Sci.* 320: 400-414.
- Zheng L, Xiaomei L, Liu J (2004). Adsorptive removal of phosphate from aqueous solutions using iron oxide tailings. *Water Res.* 38: 1381-1326.
- Zhong B, Stanforth R, Wu S, Chen JP (2007). Proton interaction in phosphate adsorption onto goethite. *J. Colloid Interface Sci.* 308: 40-48.